Sexual dimorphism and asymmetries in the gray–white composition of the human cerebrum

John S. Allen,[a,b,*] Hanna Damasio,[a] Thomas J. Grabowski,[a] Joel Bruss,[a] and Wei Zhang[c]

[a] Department of Neurology, Division of Behavioral Neurology and Cognitive Neuroscience, University of Iowa Hospitals and Clinics,
200 Hawkins Drive, Iowa City, IA 52242, USA
[b] Department of Anthropology, University of Iowa, Iowa City, IA 52242, USA
[c] Department of Biostatistics, University of Iowa College of Public Health, Iowa City, IA 52242, USA

Abstract

Using high resolution MRI scans and automated tissue segmentation, gray and white matter (GM, WM) volumes of the frontal, temporal, parietal, and occipital lobes, cingulate gyrus, and insula were calculated. Subjects included 23 male and 23 female healthy, right-handed subjects. For all structures, male volumes were greater than female, but the gray/white (G/W) ratio was consistently higher across structures in women than men. Sexual dimorphism was greater for WM than GM: most of the G/W ratio sex differences can be attributed to variation in WM volume. The corpus callosum, although larger in men, is less sexually dimorphic than the WM as a whole. Several regions demonstrate pair-wise asymmetries in G/W ratio and WM volume. Both the cingulate gyrus and insula exhibit strong asymmetries. The left cingulate gyrus is significantly larger than the right, and the G/W ratio of the left insula is significantly greater than that of the right. Although statistically significant sex differences and asymmetries are present at this level of analysis, we argue that researchers should be wary of ascribing cognitive functional significance to these patterns at this time. This is not to say, however, that these patterns are not important for understanding the natural history of the human brain, and its evolution and development.
© 2003 Elsevier Science (USA). All rights reserved.

Keywords: Brain; Volume; Lobe; Neuroimaging; MRI; Segmentation; Evolution

Introduction

Across mammal species, the relative composition of gray and white matter (GM and WM) in the (neo)cortex is remarkably uniform (Zhang and Sejnowski, 2000). Humans conform to the general mammalian trend. However, volumetric magnetic resonance imaging (MRI) studies indicate that GM and WM composition varies with sex, age, and health status. In children, GM growth outpaces WM growth during the first 2 years of life (approximately), but thereafter, WM growth predominates (although GM growth also continues into adolescence) (Courchesne et al., 2000; Matsuzawa et al., 2001; Paus et al., 2001). After the age of 50, WM volume typically decreases more quickly than GM volume; thus the GM—WM ratio increases slightly with advanced age (Miller et al., 1980; Jernigan et al., 2001). Abnormal changes in GM and WM composition have been reported in several diseases, such as schizophrenia (Gur et al., 2000; Mathalon et al., 2001) and bipolar illness (Brambilla et al., 2001). In Alzheimer's disease, prefrontal GM and WM decline at a similar rate, while in normal aging, WM reduction is typically more pronounced than GM reduction (Salat et al., 1999).

Sex differences have been reported for the GM–WM composition of the cerebrum. Earlier studies with relatively small numbers of subjects indicated that sexual dimorphism is greater for WM than GM, because significant differences in WM but not GM volumes were found (Filipek et al., 1994; Passe et al., 1997). This has been confirmed by larger studies, which have shown that while both GM and WM volumes are smaller in women than

* Corresponding author. Fax: +1-319-356-4505.
E-mail address: jsallen38@aol.com (J.S. Allen).

men, the WM difference is more pronounced, with the result that women have a higher overall proportion of GM than men (Peters et al., 1998; Gur et al., 1999). Sexual dimorphism in the GM composition of some anatomical subregions (dorsolaeral prefronal cortex and superior temporal gyrus; Schlaepfer et al., 1995) and for several gyri (Goldstein et al., 2001) has also been reported. In terms of sex differences in the overall GM–WM composition of the human cerebrum, a basic issue emerges: should the fact that women have a higher percentage of GM than men be interpreted as women having "more" GM or "less" WM? Gur and colleagues (1999) argue that the higher relative GM composition of women's brains may compensate for smaller cranial capacity, by devoting more of that space to "computation" rather than "information transfer."

To date, MRI-based studies of normal variation in GM–WM composition have focused on large sectors of the brain (hemisphere or whole) (Gur et al., 1999; Blatter et al., 1995), have been based on brains resized in the process of automated parcellation (Nopoulos et al., 2000), or have used arbitrary criteria to define regions of the brain (Pfefferbaum et al., 1994) or slice-wise sampling strategies (Raz et al., 1997). In this paper, we address sexual dimorphism and lateral asymmetry in the GM–WM volumes of the major lobes and selected gyri of the human cerebrum (frontal, parietal, temporal, and occipital lobes, and the cingulate gyrus, and insula), in a sample of 46 healthy, right-handed adults. Parcellation of the brain was based on strict neuroanatomical criteria, and regions of interest were manually traced on each slice of high resolution MRI-scans. Our results provide an anatomically robust account of sexual dimorphism and asymmetry in GM and WM composition in the major anatomical subregions of the cerebrum.

Materials and methods

Subjects

Subjects were 23 men (mean age = 32.1 years, SD = 8.8, range 22–49) and 23 women (mean age = 32.6 years, SD = 7.5, range 23–47) of European descent. All were right-handed (scores on the Oldfield-Geschwind Handedness Inventory: men, mean = +92, SD = 12.9; women, mean = +94, SD = 6.6) with no left-handedness in first-degree relatives, healthy, and with no history of neurological or psychiatric illness. All gave informed consent in accordance with institutional and federal rules. Subjects (sex and age matched) for this study were drawn from a pool of more than 240 normal volunteers for functional imaging projects. MRI scans were obtained for all these subjects as part of several unrelated PET studies.

Image acquisition

Thin cut MR images were obtained in a GE Signa scanner operating at 1.5 Tesla, using the following protocol: SPGR/50, TR 24, TE 7, NEX 1 matrix 256 × 192, FOV 24 cm. We obtained 124 contiguous coronal slices, 1.5 or 1.6 mm thick and interpixel distance 0.94 mm. The slice thickness was adjusted to the size of the brain so as to sample the entire brain, while avoiding wrap artifacts. Three individual 1NEX SPGR datasets were obtained for each brain during each imaging session. These were coregistered and averaged post hoc using Automated Image Registration (AIR 3.03, UCLA, Woods et al., 1992), to produce a single data set, of enhanced quality with pixel dimensions of 0.7 mm in plane and interslice spacing of 1.5–1.6 mm between planes (Holmes et al., 1998).

All brains were reconstructed in three dimensions using Brainvox (Frank et al., 1997), an interactive family of programs designed to reconstruct, segment, and measure brains from MR acquired images. An automated program, extensively validated against human experts (Grabowski et al., 2000), was used to segment the images into the three primary tissue types (white, gray, CSF) (Fig. 1). Before tracing regions of interest (ROIs), brains were realigned (but *not* resized) along a plane running through the anterior and posterior commissures (i.e., the AC–PC line); this ensured that coronal slices in all subjects were perpendicular to a uniformly and anatomically defined axis of the brain.

Regions of interest

Regions of interest were traced by hand on contiguous coronal slices of the brain. Anatomical landmarks were identified and marked on the surface of 3D reconstructions (see Fig. 2). The parcellation of the brain was based on a scheme modified from Rademacher et al. (1992), with additional consultation of several anatomical texts (including Ono et al., 1990; Damasio, 1995; Duvernoy, 1991); see Allen et al. (2002) for a very detailed description of the parcellation method and tracing conventions. In brief, the ROIs used in this study were traced as follows (see Fig. 3 for a sample of tracing on a single coronal slice).

Basal ganglia and hemispheres

The basal ganglia, claustrum, and thalamus were identified on coronal slices and traced in a single ROI; the value of its GM was subtracted from the frontal or parietal lobe volumes as appropriate. The cerebellum, hypothalamus, and brain stem were excluded from all tracings. The hemisphere volume is the sum of all other volumes of one side of the cerebrum (excluding the basal ganglia/thalamus/claustrum ROI).

Frontal lobe

The major sulcal boundaries of the frontal lobe are the Sylvian fissure, the central sulcus, and the cingulate sulcus
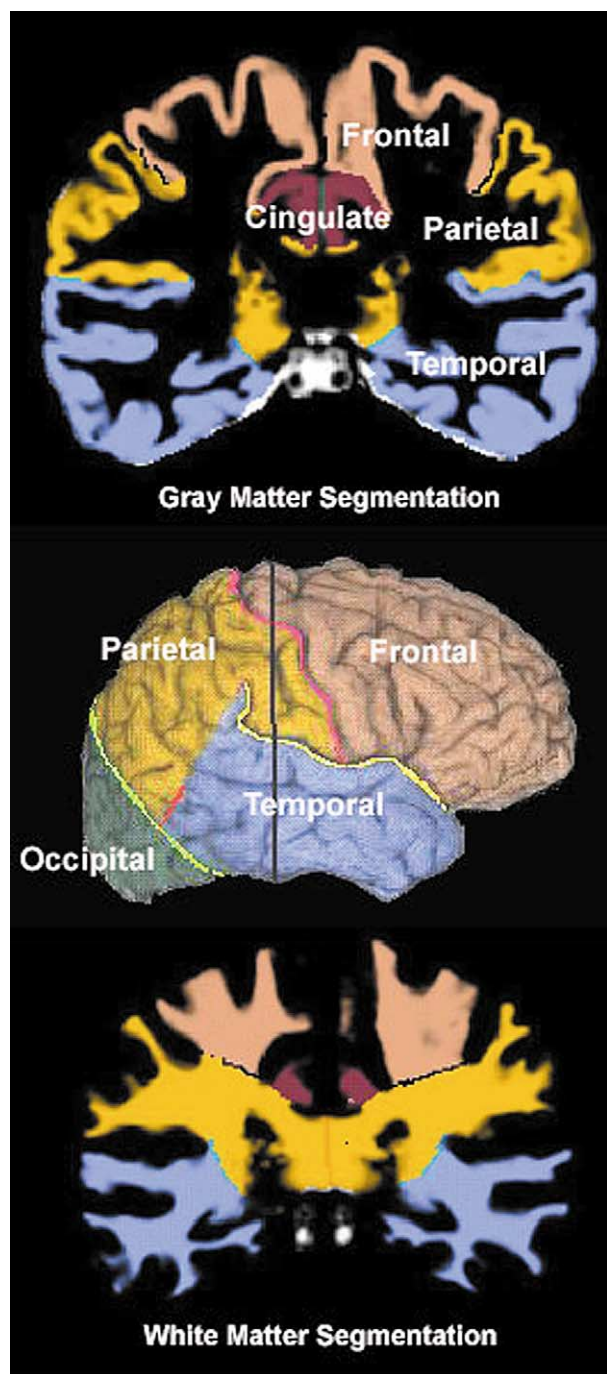
Fig. 1. Gray matter (top) and white matter (bottom) segmentation in a single coronal slice. Position of the coronal slice is indicated by the black line on the hemisphere (middle). See Grabowski et al. (2000) for more details.

Occipital cut

The occipital cut forms the anterior boundary of the occipital lobe and the posterior boundaries of the parietal and temporal lobes (Fig. 2). It is a plane defined by the following three points: the superior end of the parietooccipital sulcus (point 1) and the junction of the parietooccipital and calcarine sulci (point 2), on the mesial surface, and the preoccipital notch on the lateral surface (point 3). This plane is automatically rendered as a slice by the Brainvox image analysis program. On this slice, the appropriate hemisphere is outlined, generating the limiting line on the surface of the brain that corresponds to the "cut." In coronal
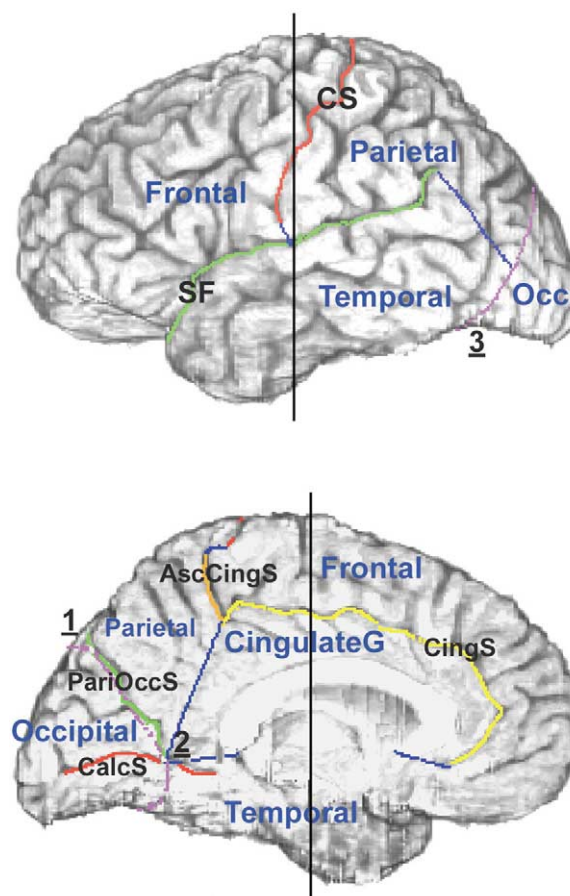

Fig. 2. Parcellation of the left hemisphere. The frontal lobe is bordered by the Sylvian fissure (SF), central sulcus (CS), cingulate sulcus (CingS), and the ascending branch of the cingulate sulcus (AscCingS). The occipital lobe is separated from the rest of the hemisphere by a plane that includes three points: 1, the superolateral extent of the parieto-occipital sulcus (PariOccS); 2, the junction of the PariOccS and the calcarine sulcus (CalcS); and 3, the occipital notch. The temporal lobe is bordered by the SF and a line drawn from the end of the SF to a point one-fourth the distance along the surface of the brain between points 3 and 1. The cingulate gyrus is limited by the CingS and an arbitrary connection starting at the junction of the CingS and AscCingS, going to the junction of the CalcS and PariOccS, and then on to the most inferior point of the splenium. The parietal lobe is defined by the CS, SF, occipital cut, and posterior limits of the temporal lobe and cingulate gyrus. See Allen et al. (2002) for more details.

(Fig. 2). The superoposterior boundary on the mesial surface is formed by the ascending branch of the cingulate sulcus and the mesial extension of the central sulcus. Because these sulci do not join, an arbitrary line linking the two is drawn along the surface of the brain in the parasagittal cut in which the end of the central sulcus is seen. The cingulate gyrus and insula are excluded from the frontal lobe.
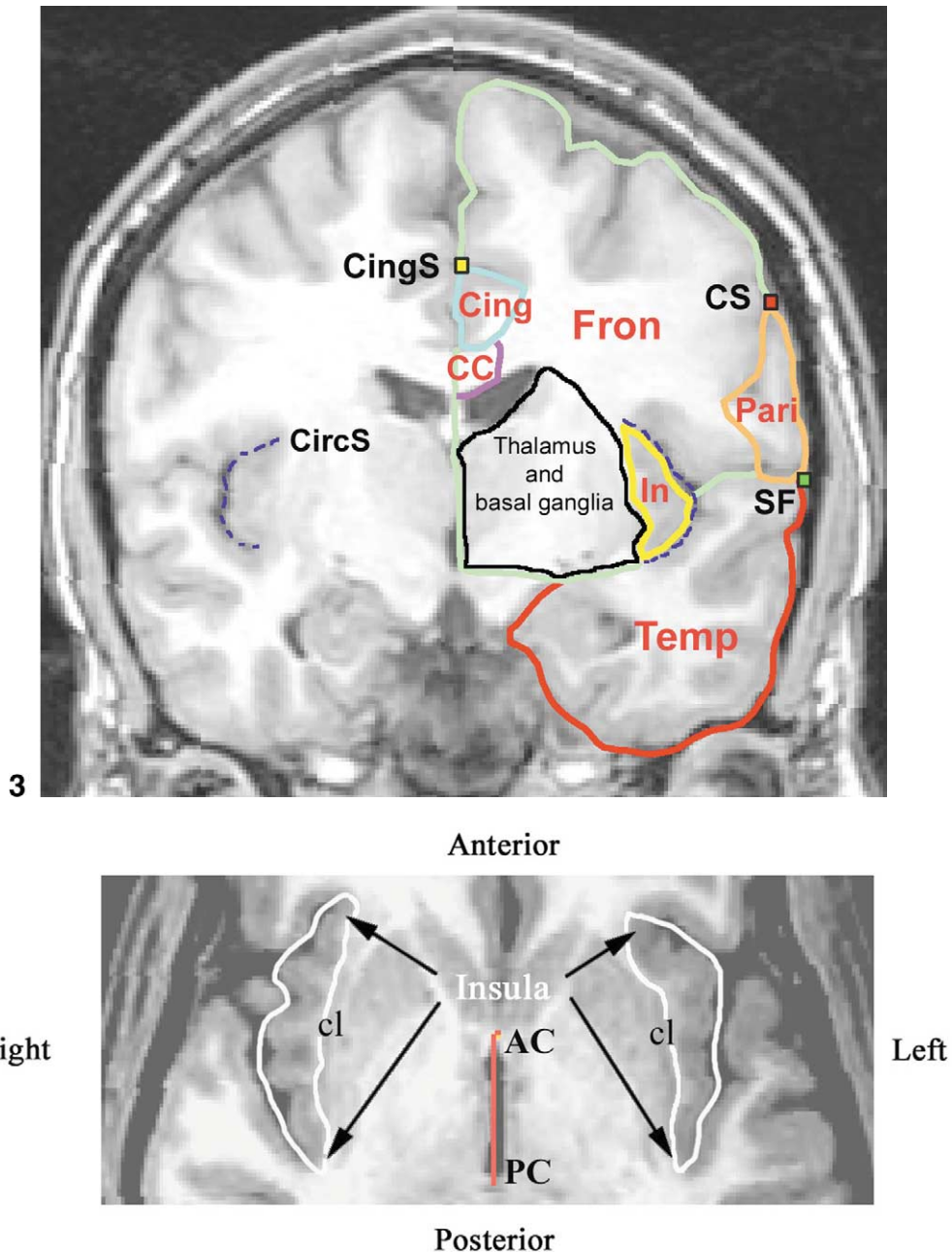
Fig. 3. Coronal slice (indicated by the black line in Fig. 2) illustrating parcellation of the left hemisphere. The ROI labeled "Thalamus and basal ganglia" is included in the frontal lobe ROI, but the gray matter of the thalamus and basal ganglia is subtracted from the total gray matter of the frontal lobe ROI.

Fig. 5. MR image illustrating asymmetry in the insula. The slice is in axial orientation cut through a line (in red) connecting the anterior and poster commissures (AC, PC). Note that the right insula is more gyrified than the left. The insula is limited laterally by the circular sulcus (white line) and mesially by the claustrum (thin, gray matter structure labeled cl).

slices, this line appears as two points on the surface of the brain.

Temporal lobe

The temporal lobe is bounded by the Sylvian fissure superiorly and the parahippocampal fissure mesially. On the mesial surface, the posterior boundaries are formed by the occipital cut and an arbitrary line drawn from the junction of the parietooccipital and calcarine sulci to the most inferior point of the splenium of the corpus callosum. On the lateral surface, the boundary between the temporal and occipital lobes is formed by the occipital cut. An additional limiting line is drawn from the end of the Sylvian fissure to a point along the lateral portion of the occipital cut. This point is one-quarter of the distance from the preoccipital notch (point 3) to the parietooccipital sulcus (point 1), as mea-

sured along the surface of the brain in the coronal slice containing the occipital cut. This line forms the boundary between the temporal and parietal lobes.

Occipital lobe

The occipital lobe is bounded by the occipital cut, with the exception of the superomesial boundary, where instead the parietooccipital sulcus is used to separate the occipital from the parietal lobe (Fig. 2).

Parietal lobe

The boundaries are the central sulcus, Sylvian fissure, ascending branch of the cingulate sulcus, occipital cut, and the arbitrary line separating it from the temporal lobe as described above (Fig. 2). The parietal lobe is separated from the posterior cingulate by a line drawn from the origin of the ascending branch of the cingulate sulcus to the junction of the parietooccipital and calcarine sulci.

Cingulate gyrus

The cingulate gyrus is bounded by the cingulate sulcus and the callosal sulcus (Fig. 2). The inferior boundary of the anterior cingulate gyrus is formed by a line drawn from the anteroinferior end of the sulcus to the posterior point of the rostrum of the corpus callosum (this corresponds to the anteroinferior end of the callosal sulcus). The posterior cingulate is separated from the parietal and temporal lobes by the two arbitrary lines described above. In cases of double cingulate sulci, the "outside" sulcus was chosen as the boundary for the gyrus.

Insula

The insula is defined by the circular sulcus, which can be clearly seen in coronal cuts (Fig. 3). Anteriorly, the insula may appear as a small amount of gray matter embedded in the surrounding tissue of the frontal lobe. The insula is separated from the rest of the hemisphere by a line linking the deepest extent of both ends of the circular sulcus. When the claustrum becomes visible, the line is edited to exclude it.

Corpus callosum

The corpus callosum was defined in coronal cuts as the white matter bounded superiorly by the callosal sulcus and inferiorly by the lateral ventricles or the third ventricle. The lateral boundaries of the callosum were formed by dropping lines straight down (perpendicular to the AC–PC line) from the depth of the callosal sulci to the ventricles (Fig. 3). The corpus callosum is included in the volumes of the frontal and parietal lobes (actually, half in each hemisphere). Surface area on the mesial surface has traditionally been used to quantify callosal size. In a previous study (Allen et al., 2002), we found that our measure of callosum volume is highly correlated ($r \sim 0.9$) with midline surface area measures of that structure. Our volumetric parcellation of the corpus callosum is more conservative than that of Meyer et

al. (1999), who extend the lateral boundaries of the callosum to the approximate depth of the cingulate sulcus rather than the callosal sulcus.

Reliability

The vast majority of ROIs were traced by one of the authors (JSA), with review and consultation with one of the other authors (HD). A reliability study was undertaken comparing the tracing of JSA with that of an expert tracer who was not otherwise involved in the project. The left frontal and occipital lobes (chosen as the least and most arbitrary of the major lobes) and the insula (the smallest and most variable structure) were traced in a random sample of 10 of the study subjects, starting with the identification of the surface landmarks (for the frontal and occipital lobes). The nonstudy tracer was allowed to consult with HD, who did no tracing herself. Parametric correlations (Pearson's) between the volumes obtained by the two tracers were $r = 0.997$ for frontal WM and $r = 0.980$ for frontal GM, $r = 0.980$ for occipital WM and $r = 0.969$ for occipital GM, and $r = 0.991$ for insula WM and 0.985 for insula GM. All of these values are highly significant ($P < .001$).

Statistical analysis

Statistical analyses were performed using SPSS for Windows (version 9.0.0) and SAS (version 8.0). Independent samples t tests were used to compare means and correlation coefficients (Pearson's) and principal components analysis were used to look at the interactions among variables. Hemispheric asymmetries were examined with pair-wise t tests and a conventional asymmetry index ($[L-R]/[L + R/2]$). Analysis of covariance (ANCOVA) and multifactor covariance analysis (MANCOVA) were used to assess the interactions among GM, WM, and total volumes and sex differences in gray–white ratio by lobe (MANCOVA results confirmed the results of the ANCOVA, so they are not presented here). Effect sizes (absolute difference of means/ pooled standard deviation) and 95% confidence intervals were used to calculate the magnitude of volume differences between sexes (Welkowitz et al. 1982). Effect sizes of 0.20 are considered "small," 0.50, "medium," and greater than 0.80 as "large." Volume determinations from ROIs were made using image analysis programs developed in our laboratory (Frank et al., 1997).

Results

The GM and WM volume measures of the hemispheres, and frontal, temporal, parietal, and occipital lobes, and the cingulate gyrus and insula, for all subjects, are presented in Appendices 1–4.

Table 1 presents the GM and WM volumes and GM–WM ratio (G/W ratio) by sex and hemisphere for all

Table 1
Volumes (cm^3) of major brain sectors, gray–white ratios, and male–female differences (effects sizes and *t* test *P* value)

Sector	Tissue	Male mean (SD)	Female mean (SD)	Mean difference (95% CI)	Effect size	*t* test *P* value
Left hemi	Gray	303.1 (27.1)	274.3 (26.5)	28.8 (12.4 to 45.2)	0.95	.001
	White	239.4 (27.7)	204.2 (21.0)	35.2 (14.7 to 45.7)	1.17	.000
	Total	542.6 (50.8)	478.4 (44.6)	64.2 (43.6 to 84.8)	1.12	.000
	G/W	1.27 (0.10)	1.35 (0.09)	0.08 (0.02 to 0.14)	0.78	.013
Right hemi	Gray	302.7 (29.6)	277.2 (27.2)	25.5 (8.1 to 42.9)	0.83	.004
	White	243.1 (28.6)	206.7 (21.4)	36.4 (21.0 to 51.8)	1.17	.000
	Total	545.7 (53.8)	483.9 (45.8)	61.8 (31.4 to 92.2)	1.04	.000
	G/W	1.25 (0.10)	1.35 (0.09)	0.10 (0.04 to 0.16)	0.94	.002
Left frontal	Gray	106.2 (12.1)	97.8 (9.5)	8.4 (1.8 to 15.0)	0.72	.012
	White	99.0 (14.7)	85.0 (8.9)	14.0 (6.6 to 21.4)	1.01	.000
	Total	205.2 (25.8)	182.8 (17.0)	22.4 (9.1 to 35.7)	0.92	.001
	G/W	1.08 (0.09)	1.15 (0.09)	0.07 (0.02 to 0.13)	0.75	.007
Right frontal	Gray	106.4 (11.4)	97.7 (9.5)	8.7 (2.3 to 15.1)	0.77	.007
	White	101.9 (14.1)	88.6 (9.2)	13.3 (6.0 to 20.6)	0.98	.000
	Total	208.3 (24.1)	186.2 (17.2)	22.1 (9.3 to 34.9)	0.94	.001
	G/W	1.05 (0.09)	1.11 (0.09)	0.06 (0.01 to 0.12)	0.65	.043
Left temporal	Gray	78.5 (8.7)	69.1 (7.0)	9.4 (4.6 to 14.2)	1.03	.000
	White	41.4 (6.9)	35.5 (3.1)	5.9 (2.6 to 9.2)	0.97	.001
	Total	120.0 (14.9)	104.6 (9.4)	15.4 (7.8 to 23.0)	1.05	.000
	G/W	1.92 (0.18)	1.95 (0.14)	0.03 (−0.11 to 0.17)	0.19	ns
Right temporal	Gray	79.3 (10.0)	68.2 (5.8)	11.1 (6.1 to 16.1)	1.13	.000
	White	43.5 (6.9)	35.4 (4.4)	8.1 (4.6 to 11.6)	1.15	.000
	Total	122.8 (16.2)	103.6 (9.4)	19.2 (11.1 to 27.3)	1.18	.000
	G/W	1.83 (0.16)	1.94 (0.17)	0.11 (0.01 to 0.21)	0.65	.030
Left occipital	Gray	29.7 (3.9)	28.3 (5.2)	1.4 (−1.4 to 4.2)	0.31	ns
	White	18.9 (3.1)	16.6 (3.8)	2.3 (0.2 to 4.4)	0.64	.032
	Total	48.5 (6.6)	44.9 (8.8)	3.6 (−1.2 to 8.4)	0.46	ns
	G/W	1.59 (0.18)	1.73 (0.17)	0.14 (0.03 to 0.25)	0.74	.010
Right occipital	Gray	31.1 (3.6)	29.4 (5.1)	1.7 (−1.0 to 4.4)	0.39	ns
	White	17.4 (3.6)	14.5 (3.5)	2.9 (0.7 to 5.1)	0.76	.000
	Total	48.5 (6.7)	43.9 (8.3)	4.6 (0.0 to 9.2)	0.59	.043
	G/W	1.83 (0.22)	2.07 (0.23)	0.24 (0.10 to 0.38)	0.95	.001
Left parietal	Gray	64.0 (6.2)	57.5 (6.7)	6.5 (2.6 to 10.4)	0.90	.002
	White	75.5 (7.9)	60.7 (7.7)	14.8 (10.0 to 19.6)	1.51	.000
	Total	136.5 (12.6)	118.2 (13.6)	18.3 (10.3 to 26.3)	1.15	.000
	G/W	.89 (0.08)	.95 (0.08)	0.06 (0.01 to 0.11)	0.70	.009
Right parietal	Gray	62.5 (7.2)	59.8 (8.7)	2.7 (−2.2 to 7.6)	0.24	ns
	White	74.2 (9.2)	63.0 (8.7)	11.2 (5.7 to 16.7)	1.41	.000
	Total	136.7 (15.3)	122.8 (16.3)	13.9 (4.3 to 23.5)	0.81	.005
	G/W	.85 (0.07)	.95 (0.08)	0.10 (0.05 to 0.15)	1.09	.000
Left cingulate	Gray	16.2 (3.0)	14.0 (2.8)	2.2 (0.4 to 4.0)	0.71	.013
	White	7.1 (1.4)	5.9 (1.0)	1.2 (0.5 to 1.9)	0.89	.002
	Total	23.4 (4.2)	19.9 (3.6)	3.5 (1.1 to 5.5)	0.83	.005
	G/W	2.31 (0.29)	2.37 (0.29)	0.06 (−0.12 to 0.18)	0.21	ns
Right cingulate	Gray	14.9 (2.7)	14.8 (2.5)	0.1 (−1.5 to 1.7)	0.04	ns
	White	4.8 (0.9)	4.2 (0.8)	0.6 (0.1 to 1.1)	0.68	.018
	Total	19.7 (3.4)	19.0 (3.2)	0.7 (−1.3 to 2.7)	0.21	ns
	G/W	3.09 (0.36)	3.52 (0.44)	0.43 (0.18 to 0.68)	0.96	.001
Left insula	Gray	8.9 (1.3)	7.5 (0.7)	1.4 (0.8 to 2.0)	1.26	.003
	White	.56 (0.2)	.45 (0.16)	0.1 (0.0 to 0.2)	0.61	.036
	Total	9.0 (1.3)	8.0 (0.8)	1.0 (0.3 to 1.7)	0.84	.002
	G/W	17.0 (6.2)	18.7 (6.1)	1.7 (−2.1 to 5.5)	0.28	ns
Right insula	Gray	8.6 (1.2)	7.5 (0.7)	1.1 (0.5 to 1.7)	0.85	.000
	White	1.19 (.35)	.93 (0.21)	0.3 (0.1 to 0.5)	0.83	.003
	Total	9.8 (1.4)	8.4 (0.8)	1.4 (0.7 to 2.1)	1.06	.000
	G/W	7.61 (1.75)	8.46 (2.24)	0.85 (−0.38 to 2.08)	0.42	ns

Note. SD, standard deviation; CI, confidence interval; G, gray; W, white; ns, not significant.

Table 2
Analysis of covariance *P* values

Sector		Controlling for total volume (gray + white)	Controlling for white matter volume	Controlling for gray matter volume
Hemisphere	L	.171	.899	.008[b]
	R	.032[a]	.508	.001[b]
Frontal	L	.091	.475	.008[b]
	R	.290	.970	.028[a]
Temporal	L	.770	.081	.507
	R	.468	.487	.081
Occipital	L	.042[a]	.147	.019[a]
	R	.008[b]	.042[a]	.002[b]
Parietal	L	.101	.832	.001[b]
	R	.000[b]	.006[b]	.000[b]

Note. Male–female differences in gray–white ratio for the major lobes controlling for total, gray matter, and white matter volumes. L, left; R, right.

[a] $P < 0.05$.
[b] $P < 0.01$.

brain regions measured. For nearly every structure, male GM, WM, and total volumes are significantly larger than female volumes. Exceptions include the gray and total volumes of the left occipital lobe, the gray volume of the right occipital lobe, the gray volume of the right parietal lobe, and the gray and total volumes of the right cingulate. In contrast to the volumes, the G/W ratios for women were consistently

and significantly higher than those for men. Exceptions were the left temporal lobe, left cingulate, and insula.

For most structures, the between-sex effect sizes for WM and GM indicate that WM shows a more profound degree of sexual dimorphism than GM. This is reflected in the higher G/W ratios found in women. To test the hypothesis that sex differences in the relative composition of GM and WM (as measured by G/W ratio) are due primarily to women having less white matter, an ANCOVA analysis was performed using sex as the factor and total, gray, and white volumes as covariates. The results of the ANCOVA are presented in Table 2. These data strongly indicate that differences in WM volume are more responsible for differences in G/W ratio than differences in GM volume. With the exception of the temporal lobe, which is not sexually dimorphic for G/W ratio, all of the major structures of the brain show a significant difference in G/W ratio even after controlling for GM volume. In contrast, only the right occipital and right parietal, structures for which women have relatively large amounts of GM compared to men, exhibit significant differences in G/W ratio after controlling for WM. It is important to note that for both of these structures, the WM effect is still more pronounced than the GM effect. In Fig. 4, plots of gray and white matter volumes vs G/W ratio are presented for the hemispheres; the male and female regression lines clearly demonstrate the more pronounced influence of WM volume in determining sex differences in G/W ratio.
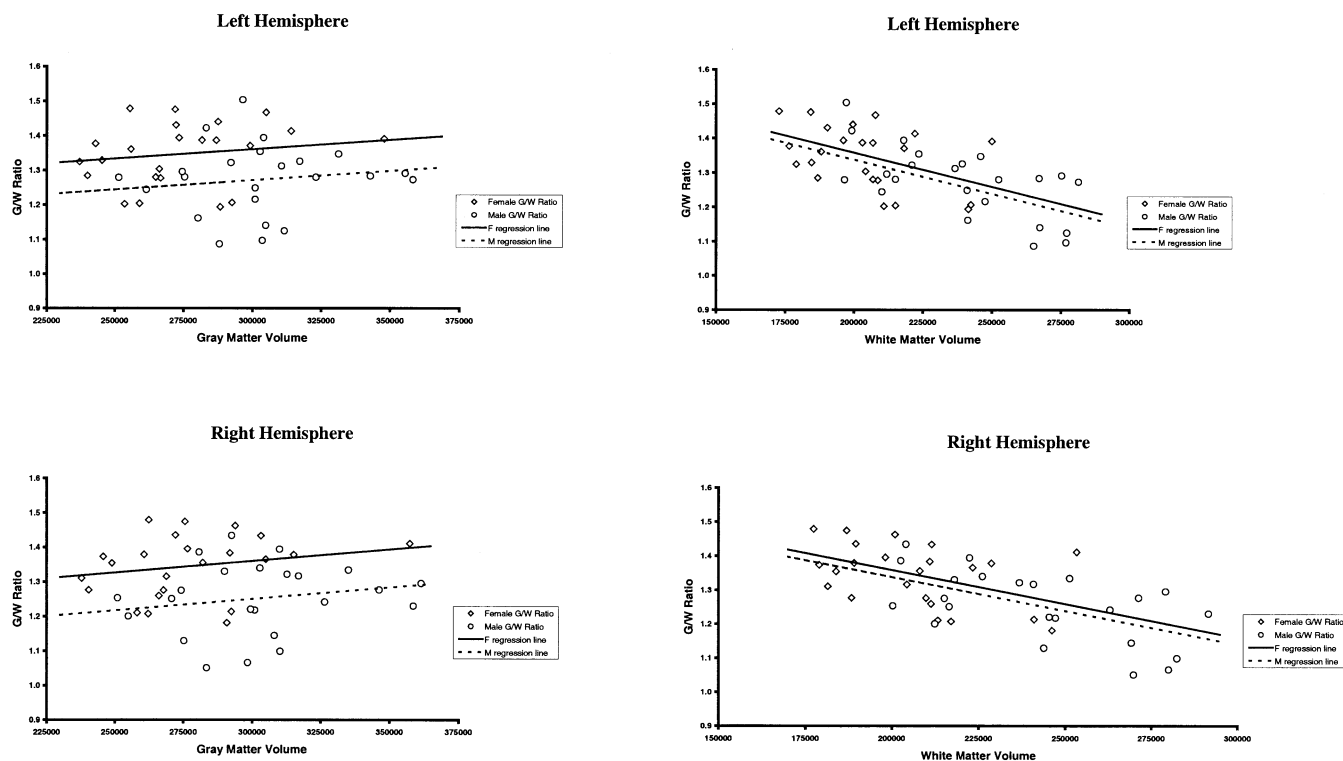

Fig. 4. G/W ratio vs gray and white matter volumes of the left and right hemispheres, for men and women.

Table 3
Corpus callosum measures

	Male mean (SD)	Female mean (SD)	Mean difference (95% CI)	Effect size	t test P value
Total volume (cm^3)	10.57 (1.62)	9.68 (1.26)	0.89 (0.14 to 1.64)	0.59	.045
CC vol./total vol.	.0097 (.0013)	.0101 (.0011)	.0004 (−.0207 to .0215)	0.33	.325
CC vol./gray vol.	.0175 (.0020)	.0176 (.0020)	.0001 (−.0219 to .0293)	0.04	.887
CC vol./white vol.	.0219 (.0028)	.0236 (.0026)	.0017 (−.0305 to .0339)	0.59	.040

Note. CC, corpus callosum; vol, volume.

Results for the corpus callosum are presented in Table 3. Male volumes are significantly greater than female volumes, although the effect size is relatively moderate compared to other parts of the cerebrum. Consistent with this is the finding that ratio of corpus callosum size to WM volume is significantly larger in women than men.

Asymmetry statistics are presented in Table 4. Using the conventional asymmetry index, the cingulate gyrus shows a pronounced leftward asymmetry. The insula is substantially larger on the right (due to WM differences), but the G/W ratio is much higher on the left. The pair-wise *t* tests indicate asymmetries in the WM composition of several structures, which are reflected in asymmetries in the G/W ratio. Men are somewhat more asymmetric for G/W ratio than women, especially in the frontal and parietal lobes.

Discussion

The results from this study provide some important refinements of our view of volumetric sexual dimorphism and GM–WM asymmetries in the human brain. Like virtually every other previous MRI study, we found that male volumes were greater than female for most cerebral structures,

ranging from the hemisphere to the insula. However, our segmentation and parcellation results indicate that sexual dimorphism in the cerebrum is not uniformly distributed across tissue types or regions.

Sex differences in G/W ratio: more gray, less white, or both?

We confirm that volume differences between the sexes are more pronounced in WM than GM. This is not only true of the entire cerebrum or hemispheres, as has been previously reported (Filipek et al., 1994; Passe et al., 1997; Peters et al., 1998; Gur et al., 1999), but it is a consistent pattern seen in all the major lobes. One previous study, using automated parcellation of resized MRI brain scans, found a relative GM increase in women only in the right parietal lobe (Nopoulos et al., 2000). Our data confirm this, with the right parietal showing the largest G/W ratio difference (in terms of statistical power) between the sexes. However, we also found that women had significantly higher G/W ratios for all structures except the left temporal lobe, left cingulate gyrus, and insula. It is likely that the automated parcellation method used by Nopoulos et al. lead to a reduction in the amount of measured volumetric variability in general (after

Table 4
Asymmetry statistics

Sector	Sex	Asymmetry index (SD)	Pair-wise *t* test *P* value			
			Gray volume	White volume	Total volume	G/W
Frontal	M	−.016 (.033)	ns	.004 (r > l)	ns	.001 (l > r)
	F	−.019 (.023)	ns	.000 (r > l)	.001 (>l)	.000 (l > r)
Temporal	M	−.023 (.091)	ns	ns	ns	.001 (l > r)
	F	.010 (.082)	ns	ns	ns	ns
Occipital	M	.000 (.152)	ns	.042 (l > r)	ns	.000 (r > l)
	F	.022 (.118)	ns	.000 (l > r)	ns	.000 (r > l)
Parietal	M	.000 (.085)	ns	ns	ns	.000 (l > r)
	F	−.036 (.061)	.016 (r > l)	.011 (r > l)	.009 (r > l)	ns
Cingulate	M	.169 (.158)	.008 (l > r)	.000 (l > r)	.000 (l > r)	.000 (r > l)
	F	.045 (.181)	ns	.000 (l > r)	ns	.000 (r > l)
Insula	M	−.077 (.061)	ns	.000 (r > l)	.000 (r > l)	.000 (l > r)
	F	−.050 (.046)	ns	.000 (r > l)	.000 (r > l)	.000 (l > r)
Hemisphere	M	−.005 (.009)	ns	.000 (r > l)	.000 (r > l)	.000 (l > r)
	F	−.011 (.007)	.000 (r > l)	.000 (r > l)	.000 (r > l)	ns

Note. Asymmetry index = [(L − R)/(L + R)/2]. M, male; F, female; SD, standard deviation; ns, not significant; G, gray; W, white; l, left; r, right.

all, the brains are resized into a common anatomical space), and one result of this is that sex differences measured using this technique are attenuated. Thus the technique identifies only the most profound "real" differences (i.e., in the right parietal) as being significant. Another study found higher G/W ratios in women in the dorsolateral prefrontal cortex and superior temporal gyrus (Schlaepfer et al., 1995), and the authors suggested that this difference might be related to verbal behavior. Given that women have higher G/W ratios than men globally, it seems premature to attribute functional significance to local patterns in the absence of G/W data about more inclusive anatomical sectors.

The G/W ratios we report (about 1.26 for men and 1.35 for women) are consistent with those reported in previous studies. For total brain or hemisphere volumes, Schlaepfer et al. (1995) reported G/W ratios of 1.16 for men and 1.21 for women, Passe et al. (1997) reported ratios of 1.15 and 1.22, Peters et al. (1998) reported 1.15 and 1.21, and Gur et al. (1999) reported ratios of 1.26 and 1.47. In the study by Goldstein et al. (2001), which is perhaps most directly comparable to ours, ratios of 1.27 for men and 1.35 for women were found (Goldstein et al. reported female gray and white cerebrum volumes that are almost identical to ours, although our males are about 5% larger). All of these results are quite consistent with one another (although Gur et al. found a greater sex difference than any of the other studies); variation in the results may be due to the different automated segmentation algorithms employed by the investigators, as well as differences in the anatomical regions of interest examined (e.g, amount of cerebellum or brain stem included in the hemisphere measures). Most of the MRI studies report a sex difference in G/W ratio; an exception is the study of Nopoulos et al. (2000) mentioned above, in which G/W ratios of about 1.47 were determined for both sexes.

Both the results of the ANCOVA analysis and the greater effect sizes for WM compared to GM point to the WM being primarily responsible for the higher G/W ratio seen in women. This is consistent with the results from a previous MRI study of whole brain volumes, which showed that after controlling for height, only the WM difference between the sexes is significant (Peters et al., 1998). In addition Gur et al. (1999) found that the slopes of the regression lines for GM volume vs cranial capacity were identical in men and women. However, the WM regression line for women had a flatter slope than the male regression line. In other words, G/W ratio increases with increased cranial capacity in women, whereas it remains steady in men. Gur et al. demonstrated that this is not simply a result of smaller cranial capacity in women. Our ANCOVA analysis is also consistent with the view that increased G/W ratio in women is not simply a function of overall smaller brain size.

In our view, these data are generally consistent with the hypothesis that the higher G/W ratio in women compared to men is due to *less white matter* in women rather than to *more gray matter*. Our interpretation is in contrast to Gur et

al.'s functional interpretation of the higher G/W ratio in women: they interpret these data as a sign of more gray matter. They argued that the higher percentage of GM in women may be an adaptation to smaller cranial size over the course of hominid evolution: women may need to devote more of their brain to computation rather than information transfer. Although this is an interesting suggestion, we have two major problems with it. First, although women have an increase in the percentage of GM, and G/W ratios are higher in women at any given brain volume, they still have less absolute GM than men. In fact, compared to histological estimates of total neuron number (Pakkenburg and Gundersen, 1997), MRI studies may lead to the underestimation of sex differences in neuronal composition. While we found about a 10% difference in GM volume between men and women, Pakkenburg and Gundersen calculated that men have 16% more neurons than women. Thus, although women are likely compensating neuronally in some way for their relatively smaller cranial capacities, it is not likely due to having "more" gray matter. Second, the significant and robust sex differences in G/W ratio are actually due to *relatively small differences* in WM composition. For example, we can estimate the relative "deficit" in WM volume in women by computing the WM mean if the effect size between men and women for WM were the same as that for GM. By adding 6.6 cc of WM to the left hemisphere and 10.6 cc to the right hemisphere, the effect sizes for gray and white matter would be the same and the G/W ratio difference between the sexes would no longer be significant. We should be wary of ascribing much functional significance to 17.2 cc of WM (about 4% of the total) distributed throughout the cerebrum.

How do we explain the sex difference in G/W ratio? Rather than looking for a particular functional explanation rooted in our recent evolutionary history, we might want to approach the problem from a broader primate perspective. For example, at the gross anatomical level, human brains are very similar to other primate brains, except that they are much larger. The proportional distribution of the brain into lobes is similar across great apes (Semendeferi et al., 1997; Semendeferi and Damasio, 2000; Allen et al., 2002), and in many primate species, females have smaller brains than males even after correcting for body size, as in humans (Holloway, 1980; Falk et al., 1999). Are sex differences in G/W ratio found in other primate species? Or is it the result of encephalization along the hominid lineage? Data on the G/W composition of other primate brains could also be very useful in elucidating endocrine effects during development that might contribute to this particular aspect of primate sexual dimorphism.

Sex differences in G/W ratio: regional patterns

Sex differences in total volume and gray–white composition are not evenly distributed throughout the cerebrum. Localized sexual dimorphism could be due to any of several

factors, including geometrical laws governing the relationship between size and shape, functional differences, or differences in hormonal exposure, with or without functional implications. Inspection of Table 1 makes it clear that there is variation in sexual dimorphism among the major lobes and sectors of the cerebrum.

In terms of total volume, the least sexually dimorphic region is the occipital lobe. Gray matter volumes for men are greater than those for women, but the difference is not significant and the effect size is relatively small. Differences in WM are also less pronounced than those seen in other regions, although WM differences are more pronounced than GM differences, thus the G/W ratio dimorphism is of a magnitude similar to that seen in other regions. There are several possible explanations for why the occipital lobe might be less sexually dimorphic than other brain regions: primary and early visual processing is not related to overall body size; as the "knob" on the end of a flattened sphere, the overall effects of larger brain size may be attenuated in the occipital region; most of the occipital lobe has relatively low levels of sex steroid receptors (Goldstein et al., 2001). It is difficult to choose among these possibilities at this time; more empirical data are clearly necessary.

Another region that has an exceptional pattern of sexual dimorphism is the temporal lobe, especially in the left hemisphere. Unlike every other region, the temporal lobe *does not* show a particularly strong difference in effect size between the GM and WM. This translates into the absence of a sex difference in the G/W ratio of the left temporal and a relatively small (but significant) difference in the right hemisphere. The temporal lobe is strongly dimorphic for volume, but why is it less dimorphic for G/W ratio? Like the occipital lobe and unlike the frontal and parietal lobes, the temporal lobe has a relatively large amount of cortical rim, which contributes to the high G/W ratio. Furthermore, our GM measures include both the amygdala and hippocampus, further increasing the G/W ratio. The GM of the temporal lobe is more dimorphic than other brain regions: males appear to have more GM than would be expected. Goldstein et al. (2001) report that males have larger amygdalae than females, even after controlling for total cerebrum size.

As mentioned above, Nopoulos et al. (2000) found that the most dimorphic region for GM percentage is the right parietal. Our results are consistent with this finding: the G/W ratio effect size for the right parietal lobe is the largest for any of the regions we measured. Effect sizes indicate that the parietal lobe as a whole is highly sexually dimorphic for WM volume. Furthermore, the right parietal lobe shows *less* sexual dimorphism for GM than other structures, which contributes to the greater difference in G/W ratio for that structure. This is consistent with another study in which it was found that the inferior parietal lobule GM volume is significantly smaller in women in the left but not the right hemisphere (Frederikse et al., 1999). Patients with Turner syndrome (X monosomy) have reduced parietal region volumes relative to total brain volume, particularly in the right

hemisphere (Reiss et al., 1995). Reiss et al. argue that this may be evidence that the structure of the right parietal in particular is influenced by X chromosome genes and/or sex steroid hormones. They had predicted that the right parietal region should be affected in Turner syndrome due to the presence of visual–spatial deficits associated with the condition. Based on sex steroid receptor densities, Goldstein et al. (2001) predicted that the inferior parietal region should have a relatively high degree of sexual dimorphism (presumably in both hemispheres). At this point, it is difficult to ascribe functional significance, if any, to the sexual dimorphism patterns observed in the parietal lobe, although several studies indicate that the right parietal lobe in particular presents an intriguing picture.

Sexual dimorphism in the corpus callosum has been intensely studied since de Lacoste-Utamsing and Holloway (1982) reported that the splenium was larger and more bulbous in women than men. In a review of this large and unwieldy literature, Bishop and Wahlsten (1997) concluded that the evidence supports the contention that the callosum is larger in men, corresponding to larger overall brain size. Recent MRI studies confirm this (Sullivan et al., 2001; Allen et al., 2002). Jäncke et al. (1997) found that corpus callosum area relative to forebrain volume is larger in women, although this may be a function of smaller brain size in general. Our results indicate that while the callosum is larger in men, the proportion of callosum volume to total white matter volume is significantly higher in women. In addition, the effect size difference between men and women for callosum volume is substantially smaller than for the rest of the WM (0.59 vs 1.17). This would indicate that the corpus callosum is less sexually dimorphic than other brain structures; in a relative sense, it is "larger" in women than men. If the effect size for corpus callosum volume were the same as for the rest of the WM, then corpus callosum/WM volume ratio would be about the same in men and women (.0219 vs .0214).

Beyond considering the functional implications (if any) of sexual dimorphism in the corpus callosum, we can also examine the structure for insights into the broader issue of sex differences in WM volume. The white matter is composed of myelinated axons (variable in size and length and organized into fiber tracts), glial cells (mostly oligodendrocytes and astrocytes), and blood vessels (Nolte, 1999; Filley, 2001). These components appear collectively in MRI scans as "white matter." The corpus callosum is one of the few white matter fiber tracts that can be seen and measured in an MRI image, and our data indicate that it is less sexually dimorphic than WM in general. The WM is obviously heterogeneous; even the corpus callosum itself is heterogenous in terms of its fiber composition and distribution (Aboitz et al., 1992; Highley et al., 1999). We suggest that WM tracts—which are essentially functional assemblages of axons—are less sexually dimorphic than other components of the WM. We know that the WM can be compressed without loss of function, as can be seen in cases

of nonsymptomatic gliomas. Analogously, the WM in women may be "compressed" relative to the WM in men, although the data on the corpus callosum suggest that WM we identify as being fiber tracts may be relatively less compressible. This is not to say that the increased G/W ratio in women is not a physiological adaptation of some kind, but again, that it may or may not be due to factors directly related to cognitive processing.

Volumetric and G/W asymmetries

Consistent with most of the post mortem literature on hemispheric asymmetries (Von Bonin, 1962; Kertesz et al., 1986; Zilles et al., 1996), we found that the right hemisphere was slightly larger than the left. Although the size difference between the hemispheres is small, within individuals, pairwise *t* tests indicate significant trends for both women and men to have more WM in the right hemisphere, and for women also to have more GM. Men had a higher G/W ratio in the left hemisphere, which is consistent with the results of Gur et al. (1999), including higher G/W ratios in the frontal, temporal, and parietal lobes, and insula. Women also had higher G/W ratios in the left frontal lobe and insula. It is important to point out (again) that G/W ratio is a function of relative GM and WM volumes, and similar asymmetries in different regions may arise via different mechanisms. In terms of total volumes, these differences are quite subtle.

It is well known that the human brain protrudes anteriorly (frontal petalia) in the right hemisphere and posteriorly in the left hemisphere (occipital petalia) (Chui and Damasio, 1980; Zilles et al., 1996). Consistent with this, our data show that both men and women tend to have more WM in the right frontal lobe and the left occipital lobe. The right frontal and left occipital lobe total volumes are slightly larger than their opposites, although the difference was significant only for the frontal lobe of women. The presence of petalia seems to correspond to increased WM but not increased GM volume. Perhaps increased sulcal depth in the hemisphere without the petalia "compensates" for the smaller overall volume. Histological studies have shown that the striate cortex (which forms the walls of the calcarine sulcus) is larger in the right hemisphere than the left (Murphy, 1985).

Patterns of asymmetry in the largest regions of the brain are unlikely to reflect functional differences between the hemispheres; the volumetric differences are far more subtle than the functional differences. This is not necessarily true for smaller structures. The most profound anatomical asymmetries we uncovered were in the two smallest structures we measured: the cingulate gyrus and the insula. In men, the left cingulate gyrus was much larger than the right, with more WM and GM in the left hemisphere and a higher G/W ratio in the right hemisphere. In women, the left cingulate was somewhat larger, with significantly more WM, leading as in men, to a higher G/W ratio in the right cingulate. It has been known for some time that the left cingulate is more frequently doubled (with a paracingulate sulcus) than the right (Von Bonin, 1962). In a

large MRI study, Paus et al. (1996a) confirmed this, finding that a paracingulate is absent in only 20% of left hemispheres compared to 37% of right; they also found that the paracingulate sulcus was more often absent in women than men (17% vs 10%; there was no gender–hemisphere interaction). Our results are consistent with the Paus et al. findings, with men definitely having a larger left cingulate, and women showing a weaker trend in this direction. Paus et al. suggest that the presence of the paracingulate may indicate expansion of Brodmann's area 32 (associated with vocalization in monkeys), a region that receives significant sensory inputs from the primary auditory cortex; the paracingulate asymmetry would then be considered analogous to asymmetry in the planum temporale. The higher G/W ratio in the right cingulate indicates that although the left cingulate is larger volumetrically—and occupies a much larger area on the cortical surface—differences between the two in numbers of neurons may not be as great. Paus et al. (1996b) found that intrasulcal gray matter (i.e., not including cortex on the mesial surface of the brain) in the anterior cingulate is greater in the right rather than left hemisphere, with the opposite pattern observed in the posterior region (it should be noted that Paus et al. defined the cingulate somewhat differently from how we did, stopping at the marginal ramus of the cingulate posteriorly, while we included a posterior region that surrounded the splenium of the corpus callosum). Although our results and those from Paus et al. (1996b) are not exactly congruent, both studies indicate that asymmetries in the cingulate gyrus may have separate WM and GM components. Further exploration of sulcal depth and GM and WM composition of the cingulate gyrus could shed some light on the general relationship between architectonic fields and gross cortical anatomy.

In terms of G/W ratio, the insula was the most asymmetric structure we measured. In both men and women, the left insula had a much higher G/W ratio than the right; this was primarily due to there being significantly less WM in the left than the right insula. Visual inspection of the insulae of our subjects confirms that it is an asymmetric structure (see Fig. 5). The right insula appears to have more and smaller gyri than the left, which seems to give the right insula a more bowed shape along the lateral surface compared to the left. This would lead to the inclusion of more WM, given that we define the medial boundary of the insula as a line linking the depths of the circular sulcus. Of course, this is a visual impression at this point and requires systematic quantitative study to confirm it. Unfortunately, a detailed reanalysis of insula anatomy does not include any information on laterality patterns (Türe et al., 1999). However, a recent voxel-based morphometry study of cerebral asymmetries did find that the anterior insular region was larger in the right hemisphere (Watkins et al., 2001).

Based on a review of the older anatomical literature, Von Bonin (1962) states that the insula is "longer and higher on the left side." We can confirm this observation. We obtained an approximate measure of asymmetry in insular length by comparing the number of ROI slices incorporating the in-

sula in each hemisphere. In women, the insula was longer in the left hemisphere in 15 cases, the same length in six cases, and longer in the right in only two cases ($\chi^2 = 11.56$, $P < 0.01$). In men, it was longer in the left in 12 cases, the same length in three cases, and longer in the right in seven cases; this distribution approached statistical significance ($\chi^2 = 5.34$, $P \sim 0.06$). The longer and flatter left insular cortex has about the same amount of GM as the more gyrified, bowed, and shorter right insular cortex. The asymmetry of the G/W ratio in the insula—which appears to be very robust by our measures—undoubtedly reflects an asymmetry in the anatomy of the region. Our result may be partially consistent with those of Watkins et al. (2001) in that there may be more GM in the right anterior region of the insula, which "compensates" for the longer left insula. Whether or not insular asymmetries correspond to functional lateralities cannot be determined until a more complete understanding of insular function is developed (Türe et al., 1999). It also remains to be determined if asymmetries in the insula may be developmentally linked to other perisylvian asymmetries, such as the well-known leftward asymmetry in the planum temporale.

Conclusion

This study provides normative data on sexual dimorphism and asymmetries in the GM and WM composition of the human brain. It demonstrates that the global parcellation of the cerebrum based on anatomical criteria yields patterns of GM and WM distribution that must be accounted for when looking at more localized distributions of these tissues. It also clearly demonstrates that the use of resized brains in MRI volumetric studies is likely to result in a substantial loss of measured variation between the sexes, as it is almost certain that there is not a constant allometric relationship between overall brain volume and the volume of its constituent parts (Kennedy et al, 1998). These data are useful as baseline data for tracking diseases that cause progressive changes in GM/WM composition. Functional correlates of these patterns should be regarded with caution. However, we emphasize that even if sex differences or asymmetries in the GM/WM composition of various brain regions cannot be linked to proximate functional processes, they are nonetheless real, and determining their ultimate origins may yield important insights into the evolution, development, and natural history of the human brain.

Appendix 1
Men, left hemisphere gray and white volume measures in cubic centimeters

Subject (age)	Hemisphere		Frontal		Temporal		Parietal		Occipital		Cingulate		Insula	
	G	W	G	W	G	W	G	W	G	W	G	W	G	W
1 M (46)	311.7	277.2	110.7	116.2	84.2	53.8	61.4	77.3	32.3	21.1	15.2	8.5	8.0	0.4
2 M (45)	304.9	267.4	108.8	114.1	82.1	49.9	65.3	76.9	26.5	17.9	14.7	8.1	7.6	0.6
3 M (43)	288.1	265.2	100.1	108.8	77.3	44.6	59.5	79.9	27.0	22.4	15.6	8.7	8.5	0.7
4 M (38)	280.3	241.4	98.7	99.8	68.7	34.6	60.7	77.3	32.0	23.2	12.2	6.4	8.1	1.1
5 M (28)	275.4	215.1	94.6	86.9	76.3	41.8	62.0	67.1	21.9	14.0	13.5	5.0	7.2	0.2
6 M (28)	317.3	239.3	110.2	93.2	85.1	44.8	70.6	77.2	28.0	17.2	14.9	6.2	8.4	0.6
7 M (42)	301.0	247.6	104.5	102.4	78.5	42.3	60.1	73.5	32.4	21.3	15.6	7.4	9.7	0.7
8 M (32)	342.9	267.2	117.0	103.7	84.8	45.9	74.1	85.7	32.6	20.9	24.8	10.5	9.5	0.5
9 M (49)	261.6	210.2	90.6	84.7	63.4	33.7	54.1	67.5	32.3	18.2	12.9	5.4	8.2	0.7
10 M (42)	292.2	221.1	101.1	91.5	80.6	41.1	60.3	64.3	24.6	16.5	16.7	7.0	9.0	0.6
11 M (23)	251.5	196.6	84.9	78.4	65.0	31.4	54.1	62.1	26.0	17.6	15.0	6.7	6.5	0.4
12 M (23)	301.0	241.1	103.7	97.6	71.3	36.2	68.5	78.0	33.2	21.9	16.2	6.7	8.2	0.7
13 M (38)	323.1	252.5	113.1	109.8	80.9	41.4	69.5	72.0	30.5	20.6	19.7	8.1	9.4	0.6
14 M (26)	296.5	197.2	103.5	83.2	70.7	30.7	67.3	62.5	30.5	14.8	16.0	5.7	8.5	0.3
15 M (32)	303.6	276.9	105.8	108.4	77.7	49.3	67.1	89.0	29.6	20.8	17.6	8.7	5.8	0.6
16 M (29)	274.6	211.9	98.1	88.0	66.2	34.1	55.4	64.8	33.4	19.1	13.9	5.4	7.6	0.4
17 M (33)	283.3	199.2	94.1	79.2	72.8	34.2	67.9	66.3	24.6	13.2	15.0	5.7	8.9	0.5
18 M (22)	358.3	281.5	144.4	142.5	93.1	48.9	56.9	59.1	34.5	22.6	17.4	7.7	11.9	0.6
19 M (23)	355.5	275.3	123.7	113.8	99.4	53.9	74.5	81.0	28.0	17.9	20.7	8.3	9.3	0.5
20 M (25)	331.4	246.0	107.6	94.2	84.2	44.0	71.8	77.3	36.6	21.1	21.1	8.5	10.1	0.8
21 M (24)	304.0	218.1	103.0	87.7	82.9	38.9	69.1	70.5	25.7	13.9	15.5	6.9	7.7	0.3
22 M (24)	310.6	236.7	114.3	99.0	77.9	35.6	62.6	73.8	34.1	22.4	12.8	5.3	9.0	0.6
23 M (24)	302.8	223.6	110.5	94.1	83.6	42.0	58.3	65.0	26.0	15.5	16.5	6.6	7.9	0.5

Appendix 2
Men, right hemisphere gray and white volume measures in cubic centimeters

Subject (age)	Hemisphere		Frontal		Temporal		Parietal		Occipital		Cingulate		Insula	
	G	W	G	W	G	W	G	W	G	W	G	W	G	W
1M(46)	310.2	282.4	108.8	123.8	84.8	58.2	60.9	76.7	32.0	17.4	15.2	5.2	8.5	1.1
2M(45)	308.2	269.3	112.1	117.3	76.1	44.5	64.5	81.5	33.9	18.9	13.7	5.6	7.9	1.4
3M(43)	283.5	269.9	97.1	111.5	71.0	42.8	59.7	81.9	33.1	26.4	13.5	5.4	9.1	2.0
4M(38)	275.3	243.8	95.8	101.3	75.3	44.1	55.4	73.6	29.6	19.5	11.0	3.8	8.0	1.6
5M(28)	274.3	215.2	98.0	88.3	73.8	39.4	55.8	68.6	24.8	13.6	14.3	4.6	7.6	0.8
6M(28)	317.1	240.9	110.6	100.2	85.1	45.1	66.1	74.6	30.7	15.3	16.4	4.7	8.3	1.0
7M(42)	301.0	247.2	106.5	102.7	84.1	48.1	63.0	77.1	25.3	13.2	12.7	4.5	9.3	1.6
8M(32)	346.3	271.4	120.0	113.8	82.8	44.9	78.7	86.6	36.1	19.6	19.0	5.4	9.7	1.1
9M(49)	254.9	212.4	86.5	87.8	60.5	33.9	51.8	65.7	35.8	19.5	13.0	4.5	7.4	0.9
10M(42)	290.0	218.1	104.8	92.9	72.1	35.5	54.4	60.6	36.5	23.2	12.5	4.5	9.7	1.4
11M(23)	251.0	200.3	88.9	81.2	67.6	37.1	50.7	63.1	27.1	15.6	9.6	2.6	7.1	0.8
12M(23)	299.5	245.4	105.2	99.7	81.5	45.2	62.4	78.5	29.4	16.6	12.8	4.5	8.1	0.9
13M(38)	326.5	263.0	117.0	117.8	87.3	49.0	61.6	71.3	32.0	17.3	18.9	6.0	9.6	1.6
14M(26)	292.6	204.1	102.1	84.9	72.9	35.3	63.2	65.0	29.5	13.3	16.3	4.5	8.7	1.0
15M(32)	298.4	280.0	103.4	109.8	64.7	39.7	72.9	100.1	35.3	23.2	16.0	5.8	6.2	1.5
16M(29)	270.8	216.6	96.0	86.6	67.0	35.5	58.1	73.2	27.7	15.4	14.4	5.1	7.5	0.8
17M(33)	280.8	202.6	92.6	84.3	84.4	42.6	52.8	58.1	26.7	12.5	15.3	4.1	9.0	1.0
18M(22)	358.7	291.6	132.4	131.4	96.6	57.6	71.1	80.1	30.8	15.7	15.9	5.1	12.0	1.7
19M(23)	361.6	279.2	128.2	120.9	102.6	55.4	68.3	78.9	31.8	15.9	21.6	6.8	9.1	1.2
20M(25)	335.2	251.3	113.6	100.8	88.7	48.4	68.5	75.6	37.1	20.0	17.5	5.1	9.9	1.5
21M(24)	310.1	222.5	109.2	91.1	81.9	38.7	68.7	74.2	28.7	13.6	13.6	4.0	8.0	0.8
22M(24)	312.9	236.8	109.2	97.7	80.9	38.9	66.5	74.5	31.8	19.5	15.7	5.2	8.7	0.9
23M(24)	302.9	226.1	108.7	97.2	81.4	41.7	62.1	67.2	30.3	14.9	12.8	4.2	7.6	1.0

Appendix 3
Women, left hemisphere gray and white volume measures in cubic centimeters

Subject (age)	Hemisphere		Frontal		Temporal		Parietal		Occipital		Cingulate		Insula	
	G	W	G	W	G	W	G	W	G	W	G	W	G	W
1 F (39)	287.5	199.6	98.0	81.8	80.9	37.9	59.2	59.3	24.6	14.9	17.4	5.5	7.4	0.2
2 F (36)	273.4	196.1	98.4	78.6	71.6	36.7	59.9	61.2	25.5	14.7	11.3	4.6	6.8	0.3
3 F (32)	272.3	190.3	95.5	76.4	65.7	32.8	62.8	60.0	23.7	13.6	17.9	7.1	6.9	0.3
4 F (26)	314.0	222.1	111.6	93.2	78.8	38.3	64.3	64.4	31.4	17.9	20.3	7.7	7.7	0.5
5 F (41)	243.0	176.4	85.4	71.6	62.2	32.1	55.5	55.8	22.4	12.2	11.3	4.3	6.2	0.3
6 F (28)	272.0	184.3	98.5	77.7	74.2	35.3	56.2	54.8	22.5	11.3	12.6	5.0	8.0	0.3
7 F (47)	266.7	208.7	93.6	81.5	61.5	31.0	60.9	69.9	30.5	19.9	12.6	5.5	7.6	0.8
8 F (32)	255.9	188.0	90.0	74.0	67.6	34.6	53.6	60.2	25.7	13.1	11.9	5.4	7.1	0.6
9 F (23)	305.0	207.8	115.7	89.7	77.5	36.5	60.7	60.6	28.2	14.8	14.8	6.0	8.1	0.3
10 F (37)	237.1	179.0	84.2	77.5	58.6	30.3	48.9	50.1	24.9	14.7	14.1	6.0	6.5	0.4
11 F (28)	281.7	203.0	101.5	88.6	73.7	36.8	56.6	56.0	25.6	13.9	16.4	7.3	7.9	0.5
12 F (24)	292.5	242.4	105.4	97.1	65.3	35.1	67.2	79.5	34.7	23.6	12.4	6.2	7.6	0.9
13 F (26)	253.6	210.9	89.2	86.8	67.2	36.4	51.1	62.9	25.4	18.2	12.4	6.1	8.3	0.5
14 F (28)	240.0	186.8	86.9	78.9	60.5	35.0	42.6	47.8	29.8	18.7	13.6	5.9	6.7	0.5
15 F (43)	264.9	206.9	90.4	85.0	68.8	35.6	54.4	62.1	28.3	17.6	15.7	6.2	7.4	0.4
16 F (24)	286.9	206.9	103.4	87.2	71.8	33.3	60.3	63.3	29.7	16.7	14.0	6.0	7.6	0.4
17 F (41)	266.2	204.2	96.8	87.3	66.1	33.7	55.4	59.4	29.3	18.5	10.9	4.9	7.7	0.4
18 F (27)	245.3	184.6	89.7	78.5	60.9	31.0	50.5	53.6	25.2	14.2	11.3	6.6	7.7	0.5
19 F (26)	299.1	218.2	107.3	88.5	73.9	39.1	56.3	61.8	40.3	23.2	12.5	5.1	8.7	0.6
20 F (42)	259.0	215.1	95.4	94.1	64.7	40.2	52.6	58.6	25.0	15.5	14.5	6.5	7.0	0.3
21 F (41)	288.3	241.5	95.6	97.9	67.9	39.9	65.1	75.3	35.6	20.8	16.3	7.3	7.9	0.3
22 F (35)	255.5	172.8	95.4	76.0	65.6	32.6	55.2	49.2	22.5	10.5	9.6	4.1	7.3	0.4
23 F (23)	347.9	250.0	120.6	107.5	85.4	41.6	73.9	70.0	39.8	23.4	18.8	6.9	9.4	0.6

Appendix 4
Women, right hemisphere gray and white volume measures in cubic centimeters

Subject (age)	Hemisphere		Frontal		Temporal		Parietal		Occipital		Cingulate		Insula	
	G	W	G	W	G	W	G	W	G	W	G	W	G	W
1 F (39)	293.9	200.9	103.1	85.4	76.8	35.8	60.7	59.8	31.3	15.7	14.1	3.3	7.9	0.9
2 F (36)	276.6	198.2	97.7	82.3	61.6	29.7	66.8	67.5	26.9	13.8	16.9	4.2	6.6	0.8
3 F (32)	272.2	189.6	97.7	81.5	62.0	29.7	65.5	60.7	26.3	12.7	13.6	4.1	7.0	0.9
4 F (26)	315.3	228.7	111.4	103.9	67.8	32.4	69.3	66.8	36.8	18.4	22.4	6.5	7.5	0.8
5 F (41)	245.8	179.0	87.5	77.5	61.7	32.1	52.6	53.3	26.5	12.3	11.2	2.9	6.3	0.8
6 F (28)	275.6	186.9	96.9	78.9	69.2	31.7	60.1	60.6	24.1	10.9	17.4	4.2	8.0	0.5
7 F (47)	266.1	211.3	94.0	90.8	69.2	36.9	56.4	63.8	26.7	14.3	12.7	4.4	7.0	1.2
8 F (32)	260.8	189.1	88.8	76.1	65.5	34.3	60.6	63.9	24.4	9.9	14.9	3.9	6.5	1.0
9 F (23)	303.2	211.5	113.9	93.9	67.7	30.2	70.3	69.6	28.2	12.7	15.5	4.2	7.6	0.9
10 F (37)	237.9	181.5	84.6	77.8	62.9	33.2	47.5	54.2	24.6	11.7	11.4	3.6	6.8	0.9
11 F (28)	282.1	208.1	100.5	93.0	70.6	34.9	64.3	63.0	25.6	11.6	13.6	4.6	7.5	0.9
12 F (24)	290.8	246.2	102.5	98.0	65.8	37.2	67.1	85.1	32.4	19.2	15.6	5.2	7.5	1.4
13 F (26)	258.2	213.3	88.2	92.8	61.8	32.3	49.5	61.1	33.1	20.1	17.4	5.7	8.1	1.3
14 F (28)	240.5	188.4	85.1	85.4	62.8	37.0	44.6	47.1	27.9	13.6	13.6	4.3	6.4	1.1
15 F (43)	267.8	209.9	93.7	88.3	67.0	35.4	56.9	67.0	30.9	15.2	12.4	3.2	7.0	0.7
16 F (24)	291.9	211.0	103.1	86.7	72.6	33.9	63.3	70.9	31.1	14.4	14.2	4.3	7.6	0.8
17 F (41)	268.9	204.3	94.0	90.2	70.1	37.5	55.5	57.5	28.0	14.4	13.8	4.0	7.5	0.9
18 F (27)	249.0	183.9	87.1	78.9	63.7	33.5	54.2	57.6	22.3	8.7	14.3	4.2	7.4	1.1
19 F (26)	305.0	223.3	107.6	95.7	74.2	42.0	61.3	60.6	39.0	20.4	14.0	3.5	8.9	1.1
20 F (42)	262.2	217.1	98.2	100.1	68.2	42.7	49.8	55.3	25.4	13.8	13.3	4.4	7.4	0.9
21 F (41)	292.5	241.0	95.7	97.3	72.9	42.2	61.2	74.4	38.0	21.1	16.6	5.1	8.2	0.8
22 F (35)	262.4	177.4	93.4	75.9	67.9	32.9	54.5	53.1	26.4	11.4	12.6	3.4	7.6	0.7
23 F (23)	357.4	253.3	121.5	107.0	86.2	46.3	83.1	77.3	39.9	17.4	17.8	4.2	9.1	1.1

References

Aboitz, F., Scheibel, A.B., Fisher, R.S., Zaidel, E., 1992. Fiber composition of the human corpus callosum. Brain Res 598, 143–153.

Allen, J.S., Damasio, H., Grabowski, T.J., 2002. Normal neuroanatomical variation in the human brain: an MRI-volumetric study. Am. J. Phys. Anthropol. 118, 341–358.

Bishop, K.M., Wahlsten, D., 1997. Sex differences in the human corpus callosum: myth or reality? Neurosci. Biobehavior. Rev. 21, 581–601.

Blatter, D.D., Bigler, E.D., Gale, S.D., Johnson, S.C., Anderson, C.V., Burnett, B.M., Parker, N., Kurth, S., Horn, S.D., 1995. Quantitative volumetric analysis of brain MR: normative database spanning 5 decades of life. AJNR Am. J. Neuroradiol. 16, 241–251.

Brambilla, P., Harenski, K., Nicoletti, M., Mallinger, A.G., Frank, E., Kupfer, D.J., Keshavan, M.S., Soares, J.C., 2001. Differential effects of age on brain gray matter in bipolar patients and healthy individuals. Neuropsychobiology 43, 242–247.

Chui, H.C., Damasio, A.R., 1980. Human cerebral asymmetries evaluated by computed tomography. J. Neurol. Neuropsychol. Psychiat. 43, 873–878.

Courchesne, E., Chisum, H.J., Townsend, J., Cowles, A., Convington, J., Egaas, B., Harwood, M., Hinds, S., Press, G.A., 2000. Normal brain development and aging: quantitative analysis at in vivo MR imaging in healthy volunteers. Radiology 216, 672–682.

Damasio, H., 1995. Human Brain Anatomy in Computerized Images. Oxford University Press, New York.

de Lacoste-Utamsing, C., Holloway, R., 1982. Sexual dimorphism in the human corpus callosum. Science 216, 1431–1432.

Duvernoy, H., 1991. The Human Brain. Springer-Verlag, New York.

Falk, D., Froese, N., Sade, D.S., Dudek, B.C., 1999. Sex differences in brain-body relationships of rhesus macaques and humans. J. Hum. Evol. 36, 233–238.

Filipek, P.A., Richleme, C., Kennedy, D.N., Caviness Jr., V.S., 1994. The young adult human brain: an MRI-based morphometric analysis. Cereb. Cortex 4, 344–360.

Filley, C.M., 2001. The Behavioral Neurology of White Matter. Oxford University Press, New York.

Frank, R., Damasio, H., Grabowski, T.J., 1997. Brainvox: an interactive, multimodal, visualization, and analysis system for neuroanatomical imaging. Neuroimage 5, 13–30.

Frederikse, M.E., Lu, A., Aylward, E., Barta, P., Pearlson, G., 1999. Sex differences in the inferior parietal lobule. Cereb. Cortex 9, 896–901.

Goldstein, J.M., Seidman, L.J., Horton, N.J., Makris, N., Kennedy, D.N., Caviness Jr., V.S., Faraone, S.V., Tsuang, M.T., 2001. Normal sexual dimorphism in the adult human brain assessed by in vivo magnetic resonance imaging. Cereb. Cortex 11, 490–497.

Grabowski, T.J., Frank, R.J., Szumski, N.R., Brown, C.K., Damasio, H., 2000. Validation of partial tissue segmentation of single-channel magnetic resonance images of the brain. Neuroimage 12, 640–656.

Gur, R.C., Turetsky, B.I., Matsui, M., Yan, M., Bilker, W., Hughett, P., Gur, R.E., 1999. Sex differences in brain gray and white matter in healthy young adults: correlations with cognitive performance. J. Neurosci. 19, 4065–4072.

Gur, R.E., Cowell, P.E., Latshaw, A., Turetsky, B.I., Grossman, R.I., Arnold, S.E., Bilker, W.B., Gur, R.C., 2000. Reduced dorsal and orbital prefrontal gray matter volumes in schizophrenia. Arch. Gen. Psychiat. 57, 761–768.

Highley, J.R., Esiri, M.M., McDonald, B., Cortina-Borja, M., Herron, B.M., Crow, T.J., 1999. The size and fibre composition of the corpus callosum with respect to gender and schizophrenia: a post-mortem study. Brain 122, 99–110.

Holloway, R., 1980. Within-species brain-body weight variability: a reexamination of the Danish data and other primate species. Am. J. Phys. Anthropol. 53, 109–121.

Holmes, C.J., Hoge, R., Collins, L., Woods, R.P., Evans, A.C., Toga, A.W., 1998. Enhancement of MR images using registration for signal averaging. J. Comput. Assist. Tomogr. 22, 324–333.

Jäncke, L., Staiger, J.F., Schlaug, G., Huang, Y., Steinmetz, H., 1997. The relationship between corpus callosum size and forebrain volume. Cereb. Cortex 7, 48–56.

Jernigan, T.L., Archibald, S.L., Fennema-Notestine, C., Gamst, A.C., Stout, J.C., Bonner, J., Hesselink, J.R., 2001. Effects of age on tissues and regions of the cerebrum and cerebellum. Neurobiol. Aging 22, 581–594.

Kennedy, D.N., Lange, N., Makris, N., Meyer, J., Caviness, V.S., 1998. Gyri of the human neocortex: an MRI-based analysis of volume and variance. Cereb. Cortex 8, 372–384.

Kertesz, A., Black, S.E., Polk, S.E., Howell, J., 1986. Cerebral asymmetries on magnetic resonance imaging. Cortex 22, 117–127.

Mathalon, D.H., Sullivan, E.V., Lim, K.O., Pfefferbaum, A., 2001. Progressive brain volume changes and the clinical course of schizophrenia in men: a longitudinal magnetic resonance imaging study. Arch. Gen. Psychiat. 58, 148–157.

Matsuzawa, J., Matsui, M., Konishi, T., Noguchi, K., Gur, R.C., Bilker, W., Miyawaki, T., 2001. Age-related changes of brain gray and white matter in healthy infants and children. Cereb. Cortex 11, 335–342.

Meyer, J.W., Makris, N., Bates, J.F., Caviness, V.S., Kennedy, D.N., 1999. MRI-based topographic parcellation of human cerebral white matter. I. Technical foundations. Neuroimage 9, 1–17.

Miller, A.K.H., Alston, R.L., Corsellis, J.A.N., 1980. Variation with age in the volumes of grey and white matter in the cerebral hemispheres of man: measurements with an image analyser. Neuropathol. Appl. Neurobiol. 6, 119–132.

Murphy, G.M., 1985. Volumetric asymmetry in the human striate cortex. Exp. Neurol. 88, 288–302.

Nolte, J., 1999. The Human Brain. Mosby, St. Louis, MO.

Nopoulos, P., Flaum, M., O'Leary, D., Andreasen, N.C., 2000. Sexual dimorphism in the human brain: evaluation of tissue volume, tissue composition and surface anatomy using magnetic resonance imaging. Psychiat. Res.—Neuroim 98, 1–13.

Ono, M., Kubik, S., Abernathey, C.D., 1990. Atlas of the Cerebral Sulci. Thieme Medical Publishers, New York.

Pakkenburg, B., Gundersen, H.J.G., 1997. Neocortical neuron number in humans: effect of sex and age. J. Comp. Neurol. 384, 312–320.

Passe, T.J., Rajagopalan, P., Tupler, L.A., Byrum, C.E., Macfall, J.R., Ranga Rama Krishnan, K., 1997. Age and sex effects on brain morphology. Prog. Neuro-Psychopharmacol. Biol. Psychiat. 21, 1231–1237.

Paus, T., Collins, D.L., Evans, A.C., Leonard, G., Pike, B., Zijdenbos, A., 2001. Maturation of white matter in the human brain: a review of magnetic resonance studies. Brain Res. Bull. 54, 255–266.

Paus, T., Otary, N., Caramanos, Z., MacDonald, D., Zijdenbos, A., D'Avirro, D., Gutmans, D., Holmes, C., Tomaiuolo, F., Evans, A.C., 1996b. In vivo morphometry of the intrasulcal gray matter in the human cingulate, paracingulate, and superior-rostral sulci: hemispheric asymmetries, gender differences and probability maps. J. Comp. Neurol. 376, 664–673.

Paus, T., Tomaiuolo, F., Otaky, N., MacDonald, D., Petrides, M., Atlas, J., Morris, R., Evans, A.C., 1996a. Human cingulate and paracingulate sulci: pattern, variability, asymmetry, and probabilistic map. Cereb. Cortex 6, 207–214.

Peters, M., Jäncke, L., Staiger, J.F., Schlaug, G., Huang, Y., Steinmetz, H., 1998. Unsolved problems in comparing brain sizes in Homo sapiens. Brain Cognition 37, 254–285.

Pfefferbaum, A., Mathalon, D.H., Sullivan, E.V., Rawles, J.M., Zipursky, R.B., Lim, K.O., 1994. A quantitative magnetic resonance imaging study of changes in brain morphology from infancy to late adulthood. Arch. Neurol. 51, 874–887.

Rademacher, J., Galaburda, A.M., Kennedy, D.N., Filipek, P.A., Caviness, V.S., 1992. Human cerebral cortex: localization, parcellation, and morphometry with magnetic resonance imaging. J. Cognitive Neurosci. 4, 352–374.

Raz, N., Gunning, F.M., Head, D., Dupuis, J., McQuain, J., Briggs, S.D., Loken, W.J., Thornton, A.E., Acker, J.D., 1997. Selective aging of the human cerebral cortex observed in vivo: differential vulnerability of the prefrontal gray matter. Cereb. Cortex 7, 268–282.

Reiss, A.L., Mazzocco, M.M.M., Greenlaw, R., Freund, L.S., Ross, J.L., 1995. Neurodevelopmental effects of X monosomy: a volumetric imaging study. Ann. Neurol. 38, 731–738.

Salat, D.H., Kaye, J.A., Janowsky, J.S., 1999. Prefrontal gray and white matter volumes in healthy aging and Alzheimer disease. Arch. Neurol. 56, 338–344.

Schlaepfer, T.E., Harris, G.J., Tien, A.Y., Peng, L., Lee, S., Pearlson, G.D., 1995. Structural differences in the cerebral cortex of healthy female and male subjects: a magnetic resonance imaging study. Psychiat. Res.: Neuroim. 61, 129–135.

Semendeferi, K., Damasio, H., 2000. The brain and its main anatomical subdivisions in living hominoids using magnetic resonance imaging. J. Hum. Evol. 38, 317–332.

Semendeferi, K., Damasio, H., Frank, R., Van Hoesen, G.W., 1997. The evolution of the frontal lobes: a volumetric analysis based on three-dimensional reconstructions of magnetic resonance scans of human and ape brains. J. Hum. Evol. 32, 375–388.

Sullivan, E.V., Rosenbloom, M.J., Desmond, J.E., Pfefferbaum, A., 2001. Sex differences in corpus callosum size: relationship to age and intracranial size. Neurobiol. Aging 22, 603–611.

Türe, U., Yaşargil, D.C.H., Al-Mefty, O., Yaşargil, M.G., 1999. Topographic anatomy of the insular region. J. Neurosurg. 90, 720–733.

Von Bonin, G., 1962. Anatomical asymmetries of the cerebral hemispheres, in: Mountcastle, V.B. (Ed.), Interhemispheric Relations and Cerebral Dominance, Johns Hopkins Press, Baltimore, MD, pp. 1–6.

Watkins, K.E., Paus, T., Lerch, J.P., Zijdenbos, A., Collins, D.L., Neelin, P., Taylor, J., Worsley, K.J., Evans, A.C., 2001. Structural asymmetries in the human brain: a voxel-based statistical analysis of 142 MRI scans. Cereb. Cortex 11, 868–877.

Welkowitz, J., Ewen, R.B., Cohen, J., 1982. Introductory Statistics for the Behavioral Sciences. Harcourt Brace Jovanovich, San Diego, CA.

Woods, R.P., Cherry, S.R., Mazziotta, J.C., 1992. A rapid automated algorithm for accurately aligning and reslicing PET images. J. Comput. Assist. Tomogr. 16, 620–633.

Zhang, K., Sejnowski, T.J., 2000. A universal scaling law between gray matter and white matter in the cerebral cortex. Proc. Nat. Acad. Sci. USA 97, 5621–5626.

Zilles, K., Dabringhaus, A., Geyer, S., Amunts, K., Qü, M., Schleicher, A., Gilissen, E., Schlaug, G., Steinmetz, H., 1996. Structural asymmetries in the human forebrain and the forebrain of non-human primates and rats. Neurosci. Biobehavior. Rev. 20, 593–605.